TOXICOLOGICAL SCIENCES **118(2)**, 564–573 (2010)
doi:10.1093/toxsci/kfq288
Advance Access publication September 23, 2010

Clearance Kinetics of Fullerene C_{60} Nanoparticles from Rat Lungs after Intratracheal C_{60} Instillation and Inhalation C_{60} Exposure

Naohide Shinohara,* Tetsuya Nakazato,†,[1] Moritaka Tamura,† Shigehisa Endoh,† Hiroko Fukui,‡ Yasuo Morimoto,¶ Toshihiko Myojo,¶ Manabu Shimada,‖ Kazuhiro Yamamoto,§ Hiroaki Tao,† Yasukazu Yoshida,‡ and Junko Nakanishi*

*Research Institute of Science for Safety and Sustainability (RISS), National Institute of Advanced Industrial Science and Technology, Onogawa 16-1, Tsukuba, Ibaraki 305-8569; †The Research Institute for Environmental Management Technology (EMTECH), National Institute of Advanced Industrial Science and Technology, Onogawa 16-1, Tsukuba, Ibaraki 305-8569; ‡The Health Technology Research Center (HTRC), National Institute of Advanced Industrial Science and Technology, Midorioka 1-8-31, Ikeda, Osaka 563-8577; §Research Institute of Instrumentation Frontier (RIIF), National Institute of Advanced Industrial Science and Technology, Higashi 1-1-1, Tsukuba, Ibaraki 305-8561; ¶Institute of Industrial Ecological Sciences, University of Occupational and Environmental Health, Iseigaoka 1-1, Yahata-nishi-ku, Kitakyushu, Fukuoka 807-8555, Japan; and ‖Graduate School of Engineering, Hiroshima University, Kagamiyama 1-4-1, Higashi Hiroshima, Hiroshima 739-8527, Japan

[1]To whom correspondence should be addressed. Fax: +81-29-861-8308. E-mail: tet.nakazato@aist.go.jp.

Received April 30, 2010; accepted August 19, 2010

Fullerene (carbon sixty [C_{60}]) has potential industrial and medical applications. In the future, people working in or residing near manufacturing facilities may be exposed to C_{60}. Therefore, quantitative data on long-term C_{60} clearance from the lungs are required. To estimate the clearance rate and deposition fraction of C_{60} from inhalation exposure, the C_{60} burden in the lungs, liver, and brain of rats was determined after intratracheal instillation and inhalation. Male Wistar rats were intratracheally instilled with different concentrations of a C_{60} suspension prepared with Tween 80 (geometric mean [GM] of particle diameter based on number, 18–29 nm; geometric standard deviation [GSD] of particle diameter, 1.5; and doses, 100, 200, and 1000 micrograms per body) or exposed to a C_{60} aerosol prepared with nebulizer (GM of particle diameter based on number, 96 nm; GSD of particle diameter, 2.0; and exposure level, 120 $\mu g/m^3$). C_{60} burden in the lungs, liver, and brain was determined at various time points (1 h to 6 months) by a newly developed sensitive high-performance liquid chromatography-ultraviolet absorptiometry combined with extraction and concentration of C_{60} from the organs. C_{60} clearance was evaluated using a 2-compartment model: fast clearance after deposition on lung surface and slow clearance after retention in the epithelium. The detection limit of our analysis method was 8.9 ng/g tissue. Pulmonary C_{60} burden decreased with time and depended on the C_{60} concentration administered. The concentration of C_{60} in the liver and brain was below the detection limit: 8.9 ng/g tissue. The half-life of intratracheally instilled C_{60} was 15–28 days. The deposition mass fraction of inhaled C_{60} was 0.14. Mode evaluation revealed that most instilled particles could be eliminated by the fast clearance pathway. This finding is consistent with the transmission electron microscopy finding that many particles were present in alveolar macrophages.

Key Words: **nano material; nanoparticle; fullerene; C_{60}; inhalation exposure; intratracheal instillation; clearance; 2-compartment model.**

Fullerene, carbon sixty (C_{60}), possesses unique physicochemical properties and is a candidate molecule for many industrial and medical nanotechnology applications, such as energy conversion and drug delivery. In the future, people working in or residing near manufacturing facilities may be exposed to airborne C_{60} particles.

Upon inhalation, some of these particles are deposited in the alveoli, depending on the particle size/shape/density, animal species, and breathing pattern. Fluid-flow models such as the multiple-path particle dosimetry (MPPD) model have been developed to estimate the deposition fraction of spherical particles in rats and humans (RIVM, 2002). The deposition fractions for rats, calculated using the MPPD model, were 0.2–0.3 for 10- to 100-nm particles and 0.05–0.2 for 100- to 1000-nm particles. In Fischer 344 rats, the deposition fraction was greater for C_{60} nanoparticles (0.14 for 55-nm particles) than for C_{60} microparticles (0.093 for 930-nm particles) (Baker *et al.*, 2008).

The rate clearance of carbon black particles from the lungs was increased with the primary particle size (14–70 nm) though the secondary particle size was similar (geometric mean [GM]: 1.4–1.6 μm) (Elder *et al.*, 2005). The main clearance pathway of particulate matter deposited on the alveolar surface is phagocytosis by the alveolar macrophages followed by transport to the larynx (Lehnert and Morrow, 1985a,b; Naumann and Schlesinger, 1986). Some particles are transferred to the pulmonary interstitium and/or epithelial cells. Total pulmonary retention and translocation to the pulmonary interstitium are significantly greater for ultrafine titanium dioxide (TiO_2) particles than for fine TiO_2 particles in rats (Oberdörster *et al.*, 1994). The size of C_{60} nanoparticles in the test suspension is very important in toxicity evaluations; however, the size of the test samples used has not been described in sufficient detail in most studies on the disposition of C_{60}. In the

Japanese New Energy and Industrial Technology Development Organization project, stable dispersion and stable aerosol of C_{60} nanoparticles (Endoh *et al*., 2009; Shimada *et al*., 2009) were successfully prepared and were applied to the pulmonary toxicity tests (Morimoto *et al*., 2010).

IP administered C_{60} particles are not detected in the brain, whereas ip or iv administered particles are detected in the liver and spleen (Bullard-Dillard *et al*., 1996; Gharbi *et al*., 2005; Moussa *et al*., 1996). In rats, iv administered C_{60} is rapidly cleared from the circulation (within 1 min), largely accumulated in the liver (90–95%), and retained in the liver for more than 120 h (Bullard-Dillard *et al*., 1996). Naota *et al*. (2009) microscopically examined aggregated C_{60} particles in the lumina of pulmonary capillaries and in pulmonary lymph nodes 5 min after intratracheal C_{60} instillation. The translocation of inhaled particles from the lung to the extrapulmonary organs has been reported to be small (< 1%, Kreyling *et al*., 2002; < 0.5%, Möller *et al*., 2008). However, Oberdörster *et al*. (2004) reported that inhaled ultrafine ^{13}C particles may be translocated to the brain (cerebrum and cerebellum) via the olfactory bulb.

Quantitative data on long-term C_{60} clearance have not yet been reported. Furthermore, although C_{60} has not been detected in brain tissue after exposure to these particles, the detection limit of the analytical methods used in previous studies was not sufficiently low. It is therefore difficult to conclude whether C_{60} nanoparticles are retained in the lung or translocated to the other organs and to determine the severity of the adverse effects of the retained particles on the basis of previous results. Highly sensitive analytical methods are required to detect the translocation of C_{60} to extrapulmonary organs, especially the brain, because unlike gaseous chemicals nanoparticles cannot be maintained at steadily high concentrations during inhalation experiments. Kubota *et al*. (2009) and Moussa *et al*. (1997) used liquid chromatography-mass spectrometry and liquid chromatography-tandem mass spectrometry, which are better than radioisotope analysis for the quantification of C_{60}, to determine the concentration of intravital C_{60}. The determination limit of these methods is 1.1 μg/g tissue (Kubota *et al*., 2009). Considering the general weight of brain (approximately 2 g), the transfer to brain cannot be detected unless more than a few percentage of the lung burden of C_{60} translocate to the brain even at high concentration such as 2 mg/m^3. Therefore, to evaluate the possibility of translocation of nanoparticle to the brain reported by Oberdörster *et al*. (2004), this limit is inadequate and more sensitive analytical methods are required. In addition, long-term clearance of C_{60} from the lung is difficult to measure because of the low C_{60} burden in the lungs in the inhalation exposure test. Therefore, in this study, we evaluated long-term C_{60} clearance by using intratracheal C_{60} instillation because this method results in a considerably greater pulmonary C_{60} burden than C_{60} inhalation.

In this study, we aimed to determine the deposition, clearance, and translocation of C_{60} nanoparticles by conducting the following experiments: (1) development of a highly sensitive method involving sample concentration and high-performance liquid chromatography (HPLC)-ultraviolet (UV) detection for the analysis of C_{60} in biological samples; (2) determination of C_{60} burden in the lung, liver, and brain until 6 months after intratracheal C_{60} instillation and until 1 month after C_{60} inhalation; and (3) estimation of the clearance rate and deposition fraction of C_{60} nanoparticles based on the results of these determinations.

MATERIALS AND METHODS

Preparation of C_{60} suspension and aerosol. To prepare a stable C_{60} nanoparticle suspension without using chemical modification or organic solvents, C_{60} (nanom purple, refined by sublimation, C_{60} purity > 99.5%, specific surface area 0.92 m^2/g; Frontier Carbon Co. Ltd, Japan) in an aqueous solution of 0.1% Tween 80 (MP Biomedicals LLC) was pulverized and dispersed in an Ultra Apex Mill (UAM-015; Kotobuki Industries Co. Ltd, Japan) according to previously described methods (Endoh *et al*., 2009; Shinohara *et al*., 2009). The GMs of particle diameter were measured by using a dynamic light scattering (DLS) technique (UPA, NIKKISO Co. Ltd, Japan). Assuming a lognormal distribution of particle diameter and spherical form of particle, these values were calculated as 18–23, 29–35, and 24–30 nm based on number, volume (weight), and surface area, respectively. The geometric standard deviation (GSD) of the distribution of the diameter was 1.5. However, it must be noted that the distribution data obtained by DLS are less reliable. The particle sizes are shown in Table 1. The ζ potentials of the aqueous suspension measured by the same instrument were –28 to –30 mV. Transmission electron microscope (TEM) image of the suspension are shown in Figures 1a and 1b.

C_{60} aerosol was prepared using a C_{60} suspension and a nebulizer by using a previously described procedure (Shimada *et al*., 2009). The size distribution and number (concentration) of aerosol particles in the exposure chamber were measured using a differential mobility analyzer (DMA) and a condensation particle counter (model 1000XP, WPS; MSP Corp.) and were found to be 96 nm (GM; GSD, 2.0 [GM and GSD of particle diameter based on number] Table 1) and 4.1×10^4 particles per cubic centimeter, respectively. The arithmetic mean ± SD in-chamber mass concentration was obtained by weighing the sampling filter and performing thermogravimetry and elemental carbon organic carbon analysis

TABLE 1
GM and GSD of Particle Diameter of C_{60}

			Number based[a]	Volume based[b]	Surface area based[c]
Suspension	Low concentration	GM (nm)	23	35	30
		GSD (—)	1.5	1.5	1.5
	High concentration	GM (nm)	18	29	24
		GSD (—)	1.5	1.5	1.5
Aerosol for exposure		GM (nm)	96	410	250
		GSD (—)	2.0	2.0	2.0

[a]Measured data from DLS (suspension) and DMA (aerosol). Note that the GSD data from DLS have low reliability.

[b]Measured data from DLS (suspension) and calculated data from the number-based diameter assuming the lognormal distribution of diameter and spherical form of particle (aerosol). Note that the GSD data from DLS have low reliability.

[c]Calculated data from the number-based diameter assuming the lognormal distribution of diameter and spherical form of particle.

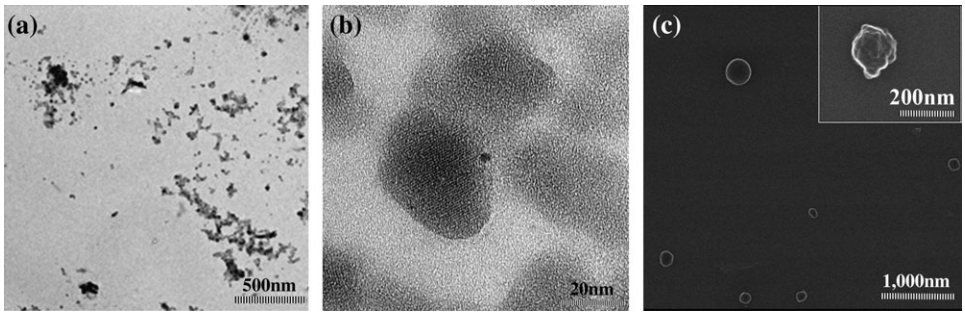

FIG. 1. TEM images of C_{60} nanoparticle suspension used for intratracheal instillation and SEM image of airborne C_{60} nanoparticles sampled using a filter and used for the inhalation experiment. (a) Spherical nanoparticles. (b) Regular ordering of fullerene molecules. (c) Airborne C_{60} nanoparticles (white).

and was found to be 0.12 ± 0.03 mg/m^3 (Morimoto *et al*., 2010). Because the aerosol particles are composed of 25% crystalline fullerene and 75% Tween 80 (Shimada *et al*., 2009), the density of each aerosol particle was calculated as 1.2 mg/cm^3. A scanning electron microscope (SEM) image of the C_{60} aerosol particles electrostatically sampled on a silicon wafer is shown in Figure 1c.

C_{60} instillation and inhalation. C_{60} particles (GM of diameter based on volume: 29–35 nm) suspended in 0.4 ml distilled water at the following doses were intratracheally instilled into male Wistar rats (age, 9 weeks): 100 μg (330 μg/kg body weight), 200 μg (660 μg/kg body weight), and 1000 μg (3300 μg/kg body weight). An aqueous solution of 0.1% Tween 80 was intratracheally instilled in 36 control rats. In each of the above four groups based on the concentration used, six rats each were dissected at 18 h (except for the 100-μg group), 3 days (only in the case of the 1000-μg group), 1 week, 1 month, 3 months, and 6 months after the instillation.

For inhalation exposure, six 9-week-old male Wistar rats were exposed to C_{60} particles (mean ± SD dose, 120 ± 30 μg/m^3; concentration, 4.1 × 10^4 particles per cubic centimeter; GM of diameter based on number, 96 nm) in whole-body exposure chamber (volume, 0.52 m^3) for 6 h/day and 5 days/week for 4 weeks. The control rats were exposed to only clean air in a same-sized chamber located in the same air-conditioned room. The rats were dissected 3 days and 1 month after the 4-week exposure period.

All procedures were conducted and all animals were handled according to the guidelines in the Japanese Guide for the Care and Use of Laboratory Animals as approved by the Animal Care and Use Committee, University of Occupational and Environmental Health, Japan, or by the Institutional Animal Care and Use Committee, National Institute of Advanced Industrial Science and Technology.

The preparation of the suspension, the exposure system, and the toxicity tests have been reported in detail in Endoh *et al*. (2009), Shimada *et al*. (2009), and Morimoto *et al*. (2010), respectively.

Analysis. Six rats in each group were anesthetized with an ip injection of pentobarbital (50 mg/kg), weighed, and dissected. In the dissection, each organ was perfused with saline after the blood drawing from the abdominal aora. The left lung, liver, and brain of five rats in each group were dissected, weighed, and cut into small pieces with scissors. The pieces were homogenized with three times their weight of saline in an electric homogenizer (Polytron RT3100; Kinematica AG, Switzerland) at 10 krpm and stored at −80°C until analysis.

The determination of C_{60} in the organs of a rat was performed by LC-UV combined with a procedure of extraction from tissue sample and concentration of C_{60} in the extracted solution. The principle of the extraction procedure of C_{60} from tissue sample is similar to those of previous study (Kubota *et al*., 2009; Moussa *et al*., 1997) but was optimized for our exposure sample, and a concentration procedure of the extracted C_{60} was added after the extraction. SDS (0.01M, 0.5 ml), acetic acid (0.1M, 0.5 ml), and toluene (HPLC grade, 5 ml) (all from Wako Pure Chemicals Co. Ltd, Japan) were added to 200 mg of homogenized tissue samples. The resultant mixture was shaken for 5 h in a shaker (SA300; Yamato Scientific Co. Ltd, Japan) and sonicated for 15 min in an ultrasonic bath (model 1510; Branson Ultrasonics Co.). The mixture was then centrifuged (Kubota 6900; Kubota Co., Japan) at 2000 × g for 10 min to separate the toluene solution, and the supernatant was collected in a test tube. The residue was shaken for 15 min with 5 ml toluene, sonicated for 15 min, and separated by centrifugation; the supernatant was collected in a test tube. The residue was shaken for 2 min with 2 ml toluene, sonicated for 15 min, and separated by centrifugation; the supernatant was collected in a test tube. Then 1 ml of toluene was gently added to the residue, and the supernatant toluene was collected in a test tube twice. Approximately 14 ml of the extracted toluene solutions (supernatants) in the test tubes were filtered with 0.2-μm filter (polytetrafluoroethylene filter media with polypropylene housing, Whatman Ltd, U.K.) to prevent the HPLC column from clogging by pieces of rat tissue, which are present at the water-toluene interface and concentrated to 0.20 ml with 0.4 ml/min of N_2 gas at 40°C by using a nitrogen concentration system (EVAN-SPE; Moritex Co., Japan).

The extracted and concentrated C_{60} and fullerene oxide (Carbon sixty oxide [$C_{60}O$]) were analyzed using an HPLC system (Shimadzu LC-10A system; Shimadzu Co., Japan) equipped with a UV detector (wavelength, 333 nm). The mobile phase was 70% (vol/vol) toluene and 30% acetonitrile (vol/vol) (Wako Pure Chemicals Co. Ltd) with a flow rate of 0.425 ml/min. The analyte (9.0 μl) was injected into a reverse phase triacontylsilyl silica (C30) packed column (particle size, 5 μm; internal diameter, 3.0 × 150 mm; Develosil RP Fullerene; Nomura Chemical Co. Ltd, Japan), which was maintained at 30°C.

After C_{60} instillation, lung tissues of the rats were observed through an energy-filtering TEM (EM922; Carl Zeiss SMT, Germany) equipped with an OMEGA energy filter. The specimen for TEM was prepared as follows. Lung tissues were fixed in glutaraldehyde and osmium tetroxide solution, dehydrated in ethanol, and embedded in epoxy resin. Ultrathin sections were cut using a diamond knife microtome. Some of the specimens were stained with 2% uranyl acetate solution and 0.5% lead citrate solution at room temperature.

Quality assurance. The detection and quantification of limits (QOL) were defined to be 3σ and 10σ of the noise level. The precision of analysis (repeatability) was checked using a standard solution of 0.024 μg/ml C_{60} in toluene ($N = 5$) and using lung tissue sample of 17 μg/g tissue C_{60}. To determine the efficiency of recovery, an aqueous suspension of C_{60} nanoparticles was spiked onto 200 mg of the lung tissues at average levels in the real samples (12–44 μg of C_{60}), the liver tissues at equal amount and 10 times amount of QOL (0.032–0.35 μg of C_{60}), and the brain tissues at equal amount and 10 times amount of QOL (0.038–0.41 μg of C_{60}) of rats.

To confirm whether the instilled suspension had evenly spread to both sides of the lung after intratracheal instillation, 10, 200, and 1000 μg of C_{60} nanoparticles in 0.4 ml distilled water were intratracheally instilled into 9-week-old male Wistar rats. At 1 h after the instillation, six rats in each group were dissected, their right and left lungs were weighed, and the concentration of C_{60} in both lungs was measured.

Deposition fraction and clearance rate constants of C_{60}. The clearance of inhaled C_{60} particles from the lung was assumed to resemble

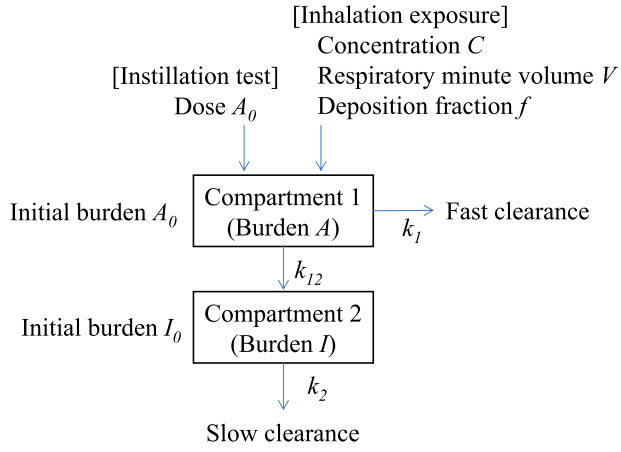

FIG. 2. Assumed compartment model for the clearance of inhaled C_{60} nanoparticles in the lung. Compartment 1 represents the alveolar surface and compartment 2 the lung interstitium or alveolar epithelial cells. Rapid clearance is attributable to phagocytosis by alveolar macrophages, transfer to the tracheobronchial region, and elimination in the sputum. Slow clearance is attributable to elimination through the lymph nodes.

a 2-compartment model (Fig. 2) described in a previous study (Kuempel *et al.*, 2001). Inhaled airborne particles are deposited on the alveolar surface, depending on their size. The amount of deposited particles is equivalent to the pulmonary burden in compartment 1. Two clearance pathways, namely, direct clearance from the lung (rapid clearance) and clearance via compartment 2 (slow clearance), were assumed to operate in this model. Particles deposited on the alveolar surface are mainly phagocytized by macrophages, transferred to the tracheobronchial region, and cleared via the sputum (Lehnert and Morrow, 1985a,b). Phagocytosis by alveolar macrophages is responsible for rapid clearance. Some of the deposited particles penetrate the epithelial cell barrier and enter the epithelial cells and some penetrate the pulmonary interstitium and are slowly cleared from the lung via the lymph nodes. These pathways are responsible for slow clearance via compartment 2. The above mechanisms can be represented by a 2-step decay rate as shown in Equations 1 and 2:

$$\frac{dA}{dt} = CVf - k_1 A - k_{12} A, \tag{1}$$

$$\frac{dI}{dt} = k_{12} A - k_2 I \quad (t = 0 : A = A_0, I = I_0), \tag{2}$$

where A is the C_{60} burden in lung compartment 1 (micrograms), C is exposure concentration (micrograms per cubic meter), V is inhalation rate (cubic meter per day), f is the deposition fraction, I is the C_{60} burden in lung compartment 2 (micrograms), A_0 is the initial C_{60} burden in lung compartment 1 (micrograms), I_0 is the initial C_{60} burden in lung compartment 2 (micrograms), and k_1, k_{12}, and k_2 are the clearance rate constants for rapid clearance (per day), translocation from compartments 1–2, and slow clearance, respectively.

In the case of C_{60} instillation, A_0, C, V, and I_0 were the instillation doses (100, 200, and 1000 μg), 0 μg/m^3, 0.27 m^3/day, and 0 μg, respectively. In the case of C_{60} inhalation, A_0, C, V, and I_0 for the nth exposure period were the burden in compartment 1 at the end of the $(n-1)$th nonexposure period a_{n-1}, 120 μg/m^3 and 0.27 m^3/day, and the burden in compartment 2 at the end of the $(n-1)$th nonexposure period i_{n-1}, respectively, and those for the nth nonexposure period were the burden in compartment 1 at the end of nth exposure period a'_n, 0 μg/m^3 and 0.27 m^3/day, and the burden in compartment 2 at the end of nth exposure period i'_n, respectively. The inhalation rate of Wistar rats (300 g), 0.27 m^3/day, was calculated from an equation given in a previous study (Bide *et al.*, 2000) for rats with an average body weight of 300 g. The decay equations for A and I were derived from Equations 1 and 2 by using Laplace transformation.

The pulmonary C_{60} burden was assumed to equal the sum of the C_{60} burden in compartments 1 and 2 $(A + I)$. The clearance rate constants k_1, k_{12}, and k_2 were estimated by fitting the decay curve of $(A + I)$ to the lung burden measured after C_{60} instillation by using the least squares method with the solver function in Microsoft Excel 2003. The deposited fraction f was estimated by fitting the decay curve of $(A + I)$ to the measured pulmonary burden after C_{60} inhalation by using the least squares method with the solver function in Microsoft Excel 2003, assuming that the clearance behavior of the inhaled particles was the same as that of the injected particles because the replacement of Tween 80 by biosurfactant could deagglomerate the inhaled agglomerated particles into the primary particles in the rat lung.

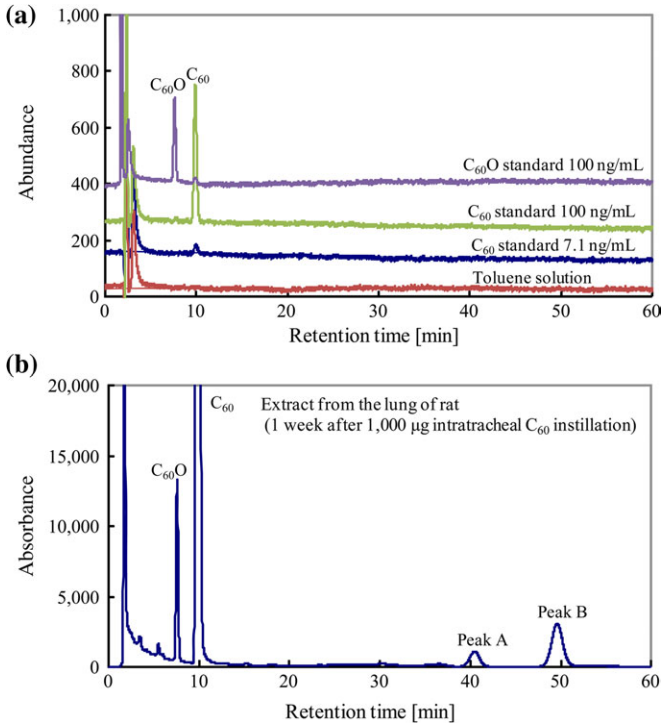

FIG. 3. Chromatogram of C_{60}. (a) Solvent (toluene), standard solution of C_{60} (100 ng/ml), standard solution of C_{60} (7.1 ng/ml), standard solution of $C_{60}O$ (100 ng/ml), and (b) sample solution extracted from the lungs of rats after intratracheal C_{60} instillation.

RESULTS

Quality Assurance

Chromatograms of toluene solution, 100 and 7.1 ng/ml of standard C_{60} solutions, and a standard $C_{60}O$ solution (100 ng/ml) are shown in Figure 3a. The detection limit and QOL were calculated to be 2.2 and 7.3 ng/ml for the standard solution, respectively. The relative standard deviation (RSD) of the results of repeated analyses of standard solution ($N = 5$) was 1.8%.

Chromatograms of the extract from the lung tissue of intratracheally instilled rat are shown in Figure 3b. The detection limit and QOL were calculated to be 8.9 and 29 ng/g

TABLE 2
Efficiency of C_{60} Recovery from Lung, Liver, and Brain Tissue

Tissue sample	Spiked amount (μg/g tissue)	Recovery efficiency (%)
Lung	11.9	98.8
	39.6	99.4
	42.8	89.9
	44.1	92.8
Liver	0.032	102
	0.354	90.3
Brain	0.038	88.8
	0.408	100

tissue for the sample tissue, respectively. The RSD of the results of repeated analysis of the tissue of C_{60} instilled rat ($N = 3$) was 3.0%. The mean ± SD efficiencies of C_{60} recovery from the lung, liver, and brain tissues was 95 ± 5, 92 ± 10, and 94 ± 6%, respectively (Table 2).

The mean ± SD pulmonary C_{60} burdens (micrograms) 1 h after the instillation were 12.4 ± 0.40, 220 ± 2.3, and 1100 ± 82 for the 10-, 200-, and 1000-μg doses, respectively. These show that 110–120% of instilled amounts were determined in the lungs. Thus, it was confirmed that most of the instilled C_{60} immediately reached the lung.

The ratio of the C_{60} burden in right or left lung to that in both lungs 1 h after the instillation (right lung, 0.311–0.396; left lung, 0.604–0.689) was almost identical to the ratio of the weight of the right or left lung to that of both lungs (right lung, 0.343–0.357; left lung, 0.643–0.657), respectively (Table 3). From these results, we concluded that the C_{60} burden after intratracheal instillation did not differ between the right and left lungs.

C_{60} Burden in the Lung, Liver, and Brain

A chromatogram of a sample solution extracted from the lung tissue of a rat is shown in Figure 3b. The lung burdens after instillation are shown in Table 4. After the instillation of 100 μg C_{60}, the mean ± SD C_{60} burdens in the entire lung (micrograms per lung) at 1 week and 1, 3, and 6 months were 70.8 ± 14, 26.5 ± 15, 5.22 ± 0.45, and 2.86 ± 2.0, respectively. In the case of the 200-μg dose, the pulmonary C_{60} burdens at 18 h and 1, 3, and 6 months were 210 ± 9.0, 62.3 ± 30, 17.3 ± 5.0, and 14.9 ± 3.1, respectively. In the case of the 1000-μg dose, the pulmonary C_{60} burden at 18 h, 3 days, 1 week, and 1, 3, and 6 months were 1000 ± 170, 1000 ± 160, 1180 ± 180, 481 ± 79, 91.4 ± 25, and 22.0 ± 6.3, respectively. C_{60} was not detected in the liver and brain after the instillation (detection limit, 0.0089 μg/g tissue). Thus, if C_{60} translocation to extrapulmonary organs does occur, the amount translocated to the liver (< 0.20 μg/liver) and brain (< 0.020 μg/brain) were confirmed to be < 0.2 and 0.02% of the instillation dose, respectively. TEM images of the alveolar macrophages in the lungs of rats at 1 week after the instillation of 0.2 milligrams per body are shown in Figure 4. Figure 4a is a low-magnification image of alveolar macrophages. Indicated arrow shown in Figure 4a is phagosome in the alveolar macrophage. Magnified image of phagosome in alveolar macrophage was shown in Figure 4b. Many black particles resembling fullerene particles are seen in the phagosome. These particles were identified as C_{60} particles because high-resolution images (Fig. 4c) show (111) lattice plane of crystalline fullerene. TEM images of the alveolar macrophages in the lungs of rats at 6 months after the instillation of 0.2 milligrams per body were shown in Figure 4d. It is difficult to see the fullerene particles in the alveolar macrophages at 6 months after the instillation. We think that most of fullerene particles are exhausted. C_{60} nanoparticles were also observed in the cytoplasm of the epithelial cells of the lung. We could not, however, confirm their presence in the pulmonary interstitium.

The lung burdens after inhalation exposure are shown in Table 5. The mean ± SD pulmonary C_{60} burdens (micrograms per lung) 3 days and 1 month after the inhalation experiment were 9.92 ± 2.2 and 5.36 ± 1.2, respectively. C_{60} was not detected in the liver and brain after inhalation exposure (detection limit, 0.0089 μg/g tissue). The TEM images of the alveolar macrophages in the lungs of rats at 3 days after inhalation exposure are shown in Figure 5. Phagosomes were

TABLE 3
Mean ± SD of the Ratio of C_{60} Burden in Each Lung to Total Lung and Each Lung Weight to Total Lung Weight at 1 h after the Instillation

C_{60} administration amount (μg)	Ratio of C_{60} burden in each lung to total lung		Ratio of weight of each lung to total lung	
	Left lung	Right lung	Left lung	Right lung
10	0.396 ± 0.076	0.604 ± 0.076	0.351 ± 0.002	0.649 ± 0.002
200	0.311 ± 0.003	0.689 ± 0.003	0.343 ± 0.009	0.657 ± 0.009
1000	0.389 ± 0.041	0.611 ± 0.041	0.357 ± 0.015	0.643 ± 0.015

TABLE 4
Lung Burden of C_{60} after Intratracheal Instillation

Time after instillation (day)	Lung burden of C_{60} (μg)		
	100 μg Instillation	200 μg Instillation	1000 μg Instillation
0.75	—	210	1000
3.0	—	—	1000
7.0	70.8	—	1180
30	26.5	62.1	481
90	5.22	17.3	91.4
180	2.86	14.9	22.0

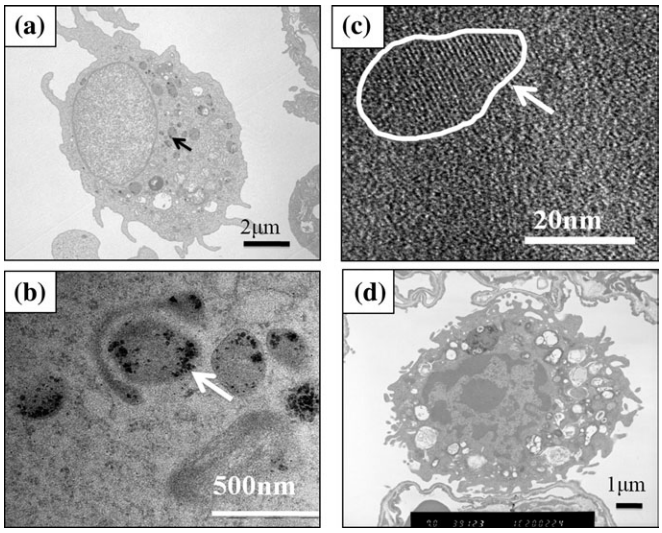

FIG. 4. TEM images of alveolar macrophage instilled with C_{60} (0.2 milligrams per rat). (a) Low-magnification image of alveolar macrophage after 1-week instillation exposure. (b) Magnified image of phagosome in alveolar macrophage after 1-week instillation exposure. Many black particles resembling fullerene particles are seen in the phagosome. (c) High-resolution image of the black particles in (b). A crystal lattice order can be observed. (d) Low-magnification image of alveolar macrophage after 6 months instillation. Few fullerene particles can be seen.

observed in the alveolar macrophages and (111) lattice plane of crystalline fullerene.

Clearance Rate Constant and Deposition Fraction of C_{60}

By fitting the decay curves of the pulmonary C_{60} burden estimated using a 2-step decay rate equation (Equations 1 and 2) until 6 months after instillation to the measured pulmonary C_{60} burden, we obtained the clearance rate constants k_1, k_{12}, and k_2 to be 0.029–0.047, 0.00044–0.0034, and 0–0.0042 per day, respectively (Table 6). The measured data and fitting curve are shown in Figure 6a. On the basis of the decay rate equations, we calculated the half-life and 90% decay period as 15, 17, and 28 days and 58, 77, and 87 days for 100, 200, and 1000 μg administration, respectively. The deposition fraction of C_{60} particles in the intratracheal instillation was assumed to be 100%; this was confirmed on the basis of the mean pulmonary C_{60} burden (micrograms) at 1 h after the instillation in the quality assurance tests.

TABLE 5
Lung Burden of C_{60} after Inhalation Exposure

	Lung burden of C_{60} (μg)
Time after last exposure (day)	120 μg/m^3 exposure
3.0	10.1
30	5.08

The pulmonary C_{60} burden after the inhalation experiment was also estimated using the 2-step decay rate equation. Assuming that the clearance behavior of the inhaled particles was the same as that of the injected particles and by fitting the decay curves of the estimated pulmonary C_{60} burden using the clearance rate constants for the rats administered 100 μg C_{60} to the measured pulmonary C_{60} burden, the deposition fraction of C_{60} particles (GM and GSD of particle diameter based on number, 96 nm and 2.0, respectively) after inhalation was estimated to be 0.14. The measured data and fitting curve are shown in Figure 6b.

Except C_{60}, three compounds ($C_{60}O$ [retention time {RT} = 7.6 min], peak A [RT = 40.5 min], peak B [RT = 49.6 min]) were observed in the extract of the lung tissue of intratracheally instilled rat (Fig. 3b). Peak A and peak B could not be identified. The ratio of $C_{60}O/C_{60}$ concentration increased from 2.2% at 3 days after the instillation to 5.0% at 3 months after the instillation; the ratio of $C_{60}O/C_{60}$ concentration in the C_{60} suspension was 2.6% (Fig. 7a). The ratio of an unidentified compound (peak A in Fig. 3b) to the C_{60} area also increased during 3 months (Fig. 7b). However, the ratio of another unidentified compound (peak B in Fig. 3b) to the C_{60} area decreased during 6 months (Fig. 7c).

DISCUSSION

In the present study, the extraction and concentration procedure of C_{60} from tissue improved the QOL to be considerably lower levels of intravital C_{60} (0.029 μg/g tissue) than those measured in a previous study (1.1 μg/g tissue; Kubota *et al.*, 2009). The low QOL of our method enabled the evaluation of long-term C_{60} clearance (at 6 months and 1 year) when the amount of pulmonary C_{60} burden was small. The precision and recovery with this method were also adequate to determine the C_{60} mass burden.

In terms of the deposition fraction of C_{60} particle, Baker *et al.* (2008) reported that the deposition fraction (count median diameter of C_{60} particles, 55 nm; GSD, 1.48) was 0.14. This value is possible to be an underestimation because their study did not take into account C_{60} clearance during exposure. The deposition fraction of C_{60} nanoparticle obtained in their inhalation test was reanalyzed using the clearance rate constants obtained in this study and the inhalation rate reported in the study of Baker *et al.* (2008), 140 ml/min, and found this fraction to be 0.18 (Fig. 6b). Therefore, the underestimation was considered to be negligible. In addition, the deposition fractions of particles with median diameters of 55 nm (GSD, 1.48; density, 1.7 g/cm^3) and 96 nm (GSD, 2.0; density, 1.2 g/cm^3) were estimated using an MPPD model with the following parameters: model in MPPD, Asymn Multipath; breathing frequency of rat, 102 breaths per minute; tidal volume of rat, 1.37 ml (Fischer 344 rats) or 1.84 ml (Wistar rats); and breathing type, nasal. In the present study, the

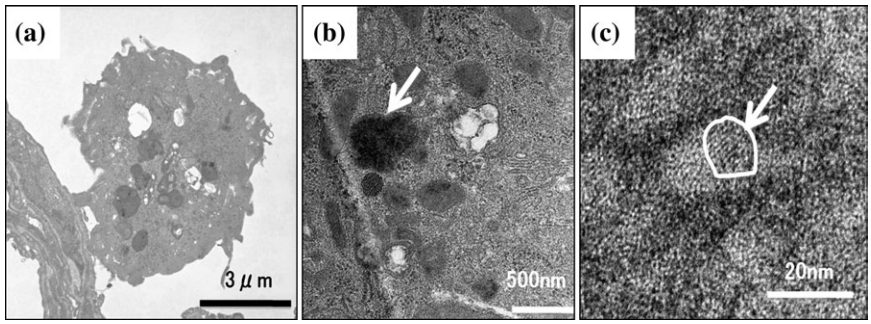

FIG. 5. TEM images of alveolar macrophage after the inhalation exposure to C_{60}. (a) TEM image of alveolar macrophage after 3 days. (b) TEM image of phagosome in alveolar macrophage after 3 days. (c) High-resolution TEM image of (b). Lattice of C_{60} particle was observed.

deposition fractions of the C_{60} nanoparticles (diameters, 55 and 96 nm) were estimated to be 0.18 and 0.14, respectively, which were higher than those calculated using the MPPD model for spherical particles (0.12 and 0.078, respectively). In the present study, the clearance rates were assumed to be same as that during the instillation test (GM, 31 nm), regardless of the particle size. The clearance rates of smaller particles (GM, 31 nm) are higher than those of larger particles (GM, 55 and 96 nm); this difference can be explained. By using the deposition fraction calculated using the MPPD model, k_1 for the 55- and 96-nm particles were approximately 1/10 of the k_1 for the 31-nm particle. According to previous studies (Madl *et al.*, 1998; Oberdörster *et al.*, 1994), the clearance rate of smaller particles might be lower than that of larger particles, but it cannot be higher than that of larger particles. Thus, this difference might be because of a reason other than the assumption regarding different clearance rates among different particle size. It may be because a small number of large particles have a skewed lognormal distribution in the MPPD model; such particles were not present in the air used for experimental exposure because the deposition fraction of these large particles is small. Thus, of models such as MPPD may lead to the over- or underestimation of deposition fractions if the particle size distribution is not carefully selected.

Xu *et al.* (2007) reported that nonaqueous $C_{60}(OH)_x$ ($x = 22$ or 24) nanoparticles were not detected in the brains of rats that were intratracheally instilled with C_{60} particles—a finding similar to that of the present study. In contrast, Oberdörster *et al.* (2004) concluded that in rats, inhaled nanoparticles deposited on the nasal mucosa are translocated to the brain via the olfactory bulb because they detected ^{13}C in the olfactory bulb, cerebellum, and cerebrum until 7 days after inhalation exposure (for 6 h) to ^{13}C-labeled carbon nanoparticles (count median diameter, 37 nm; GSD, 1.66; concentration, 170 μg/m^3). In the present study, C_{60} was not detected in the brain (< 0.020 micrograms per brain) even though rats were exposed to similar concentrations (count median diameter, 96 nm; GSD, 2.0; C_{60} concentration 120 μg/m^3) of C_{60} particles for longer durations (5 days/week for 4 weeks). Because the particles in the Oberdöster's test were generated from electric spark discharge generator, the particle in that study included much smaller particles than that in the present study. The discrepancy between the translocation results of the two studies may be because of the smaller particle size.

TABLE 6
Clearance rate constants Estimated on the Basis of the Lung Burden Measured in the Present Study

	Dose of C_{60} administered		
Clearance rate constant	100 μg	200 μg	1000 μg
K_1 (/day)	0.047	0.043	0.029
K_2 (/day)	0.0042	~0	~0
K_{12} (/day)	0.0028	0.0034	0.00044

The half-life of 55-nm-wide C_{60} particles calculated using the 1-compartment model reported by Baker *et al.* (2008) was similar to that calculated using the 2-compartment model and the data obtained in the present study. This suggests that the 1- and 2-compartment models yield similar short-term clearance estimates until 50% decrease, including exposure duration. In the present study, we first used a 1-compartment model to fit the experimental data because there were few data points and parameters. However, this model was found to be unsuitable for the estimation of lung burden between 90 and 180 days (Fig. 6a). Hence, a 2-compartment model and three clearance rate constants were used to fit the experimental data. On the basis of the 2-compartment model simulation, more than 90% of the instilled C_{60} particles were estimated to have been eliminated via the rapid clearance pathway. Thus, for the C_{60} nanoparticles, we concluded that phagocytosis by macrophages, migration of the macrophages to the trachea and bronchi, and subsequent tracheobronchial clearance was the major clearance pathway. The slow clearance rate constant k_2 was estimated to be quite low (0–0.0042). At 6 months after instillation, more than 99% of the lung burden was estimated to be in compartment 2. These results suggest that some of the instilled C_{60} nanoparticles (< 10%) are retained in the alveolar epithelial cells for prolonged periods because C_{60} nanoparticles

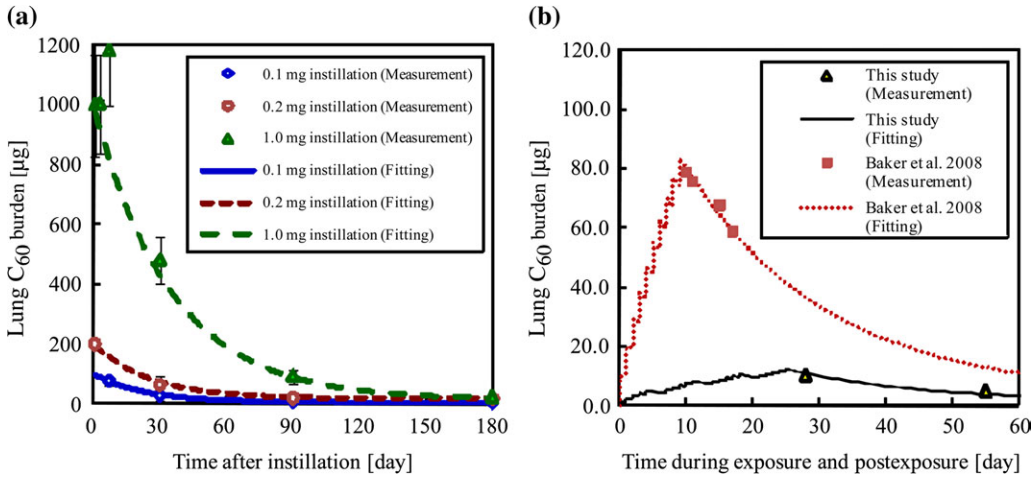

FIG. 6. Pulmonary C_{60} burden against time elapsed after (a) instillation and (b) inhalation.

were not observed in the pulmonary interstitium but in the cytoplasm of alveolar epithelial cells with the TEM observation. Alveolar macrophages are not efficient in phagocytizing nanoparticles and may not be as involved in the pulmonary retention and clearance of nanoparticles as they are in those of larger particles (Kreyling *et al.*, 2005; Oberdörster, 1993). Naota *et al.* (2009) reported that intratracheally instilled C_{60} nanoparticles were not observed in the alveolar macrophages but in the lymph nodes. In the present study, however, C_{60} nanoparticles were observed in both alveolar macrophages and alveolar epithelial cells.

Pulmonary particle overload has been observed in rats, with a particle burden of nearly 1000 μg/g tissue and delayed clearance from the lungs (Borm *et al.*, 2000; Muhle *et al.*,

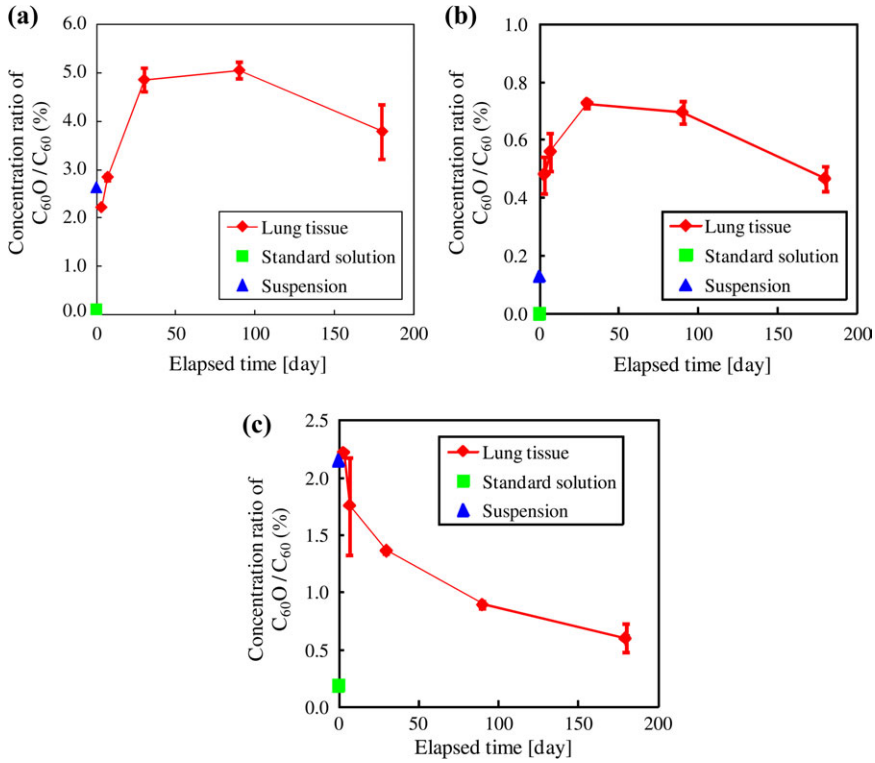

FIG. 7. Changes in the ratio of C_{60} derivatives to C_{60} with time. (a) $C_{60}O$. (b) Unidentified peak A. (c) Unidentified peak B.

1990). Because the lung weights of rats were approximately 1.3 g in the present study, the highest dose (1000 μg) administered in this study can be considered equivalent to the overload dose in previous studies. Such an overload may explain why the clearance rate of these particles was lower in the case of the 1000-μg dose than in the case of the 100 and 200-μg doses in this study. However, even if overload was induced in the rat lungs in the present study, the half-life of C_{60} in the rat lungs in the present study was shorter than half-life of carbon black particles in rat lungs reported in Elder *et al.* (2005) (GM, 14–70 nm; 64 days). Thus, it can be concluded that early stage of C_{60} nanoparticle clearance, at least, is quite rapid.

Bullard-Dillard *et al.* (1996) iv injected Sprague-Dawley rats with ^{14}C-labeled C_{60} and found that C_{60} was rapidly cleared from the blood circulation (within 1 min), and more than 90% of the injected C_{60} was accumulated in the liver. Therefore, in the present study, we concluded that the translocation of C_{60} from the lung to other organs via blood circulation was negligible because C_{60} was not detected in the liver (< 0.20 micrograms per liver). Naota *et al.* (2009) observed C_{60} particles in the lumina of the pulmonary alveoli of mice 5 min after intratracheal C_{60} instillation. Polystyrene latex particles (diameter, 240 nm) and TiO_2 particles (diameter, 22 nm) have also been observed in the alveolar lumina of rats subjected to intratracheal instillation and inhalation of these particles (Geiser *et al.*, 2005; Kato *et al.*, 2003). In the above studies, only a small population of nanoparticles can be considered to have been microscopically observed because only very small particles penetrate the alveolar-capillary barrier (Xu *et al.*, 2007).

Three compounds ($C_{60}O$, unidentified peak A, and unidentified peak B) were detected in the extract from the lung tissue of intratracheally instilled rat. The ratio of $C_{60}O$ concentration to C_{60} concentration in the lung tissues increased until 1 month after instillation and then slightly decreased until 6 months after instillation. Similar change in the ratio was also observed for the unidentified compound represented by peak A. The change in ratio may have been caused by two reasons: differences in the clearance rates of $C_{60}O$ and C_{60} or the possibility that $C_{60}O$ is a metabolic product of C_{60}. The ratio of the concentrations of the unidentified compound represented by peak B to the C_{60} in the lung tissues decreased over 6 months. This suggests that this unidentified compound (peak B) was more rapidly cleared than C_{60}. The clearance rates of $C_{60}O$ and the other unidentified compound (peak A) may be slower than those of C_{60}, or C_{60} may be metabolized to $C_{60}O$ and/or to the unidentified compound represented by peak A. Hamano *et al.* (1995) reported that C_{60} was oxidized by the synthetic cytochrome P-450 chemical model system; however, Bullard-Dillard *et al.* (1996) did not detect $C_{60}O$ in rat tissues. If C_{60} is metabolized to $C_{60}O$ and/or to the unidentified compound represented by peak A, the amount metabolized is quite small.

In this study, a sensitive analytical method for C_{60} was developed. In addition, a stable suspension of C_{60} nanoparticles with a narrow particle size distribution (GSD, 1.5) was prepared by using a surfactant without organic solvents and then characterized in detail. The following conclusions related to C_{60} nanoparticles can be reliably reached on the basis of the results: (1) The experimentally obtained deposition fraction of C_{60} nanoparticles corresponds to that calculated by using previously published models such as the MPPD model (RIVM, 2002). (2) The C_{60} nanoparticles deposited on the lung surface could be mainly cleared via phagocytosis by macrophages and tracheobronchial clearance. (3) A small percentage of the C_{60} nanoparticles deposited on the lung surface could be retained in the epithelial cells for prolonged periods. (4) No translocation of inhaled C_{60} nanoparticles to extrapulmonary organs, e.g., brain and liver, was recognized by the proposed sensitive analytical method.

FUNDING

Grant "Evaluating risks associated with manufactured nanomaterials" from the New Energy and Industrial Technology Development Organization of Japan (no. P06041).

ACKNOWLEDGMENTS

Conflict of interest: This paper is not being considered for publication in any other journal. Further, it has not been published elsewhere in part or in entirety. All the authors of the manuscript have read it, attest the validity of its contents, and agree on its submission to *Toxicological Sciences*. It should be mentioned that none of the authors have any competing interests to declare.

REFERENCES

Baker, G. L., Gupta, A., Clark, M. L., Valenzuela, B. R., Staska, L. M., Harbo, S. J., Pierce, J. T., and DillInhalation, J. A. (2008). Inhalation toxicity and lung toxicokinetics of C_{60} fullerene nanoparticles and microparticles. *Toxicol. Sci.* **101,** 122–131.

Borm, P. Y. A., Costa, D., Castranova, V., Donaldson, K., Driscoll, K., Dungworth, D., Green, F., Greim, H., Harkema, J., Jarabek, A., *et al.* (2000). The relevance of the rat lung response to particle overload for human risk assessment: a workshop consensus report. *Inhal. Toxicol.* **12,** 1–17.

Bullard-Dillard, R., Creek, K. E., Scrivens, W. A., and Tour, J. M. (1996). Tissue sites of uptake of ^{14}C-labeled C_{60}. *Bioorg. Chem.* **24,** 376–385.

Bide, R. W., Armour, S. J., and Yee, R. (2000). Allometric respiration/body mass data for animals to be used for estimates of inhalation toxicity to young and adult humans. *J. Appl. Toxicol.* **20,** 273–290.

Elder, A., Gelein, R., Finkelstein, J. N., Driscoll, K. E., Harkema, J., and Oberdörster, G. (2005). Effects of subchronically inhaled carbon black in three species. I. Retention kinetics, lung inflammation, and histopathology. *Toxicol. Sci.* **88,** 614–629.

Endoh, S., Maru, J., Uchida, K., Yamamoto, K., and Nakanishi, J. (2009). Preparing samples for fullerene C_{60} hazard tests: stable dispersion of fullerene crystals in water using a bead mill. *Adv. Powder Technol.* **20,** 567–575.

Geiser, M., Rothen-Rutishauser, B., Kapp, N., Schürch, S., Kreyling, W., Schulz, H., Semmler, M., Hof, V. I., Heyder, J., and Gehr, P. (2005). Ultrafine particles cross cellular membranes by nonphagocytic mechanisms in lungs and in cultured cells. *Environ. Health Perspect.* **113,** 1555–1560.

Gharbi, N., Pressac, M., Hadchouel, M., Szwarc, H., Wilson, S. R., and Moussa, F. (2005). [60]Fullerene is a powerful antioxidant in vivo with no acute or subacute toxicity. *Nano Lett.* **5,** 2578–2585.

Hamano, T., Mashino, T., and Hirobe, M. (1995). Oxidation of [60]fullerene by cytochrome-P450 chemical-models. *J. Chem. Soc. Chem. Commun.* **15,** 1537–1538.

Kato, T., Yashiro, T., Murata, Y., Herbert, D. C., Oshikawa, K., Bando, M., Ohno, S., and Sugiyama, Y. (2003). Evidence that exogenous substances can be phagocytized by alveolar epithelial cells and transported into blood capillaries. *Cell Tissue Res.* **311,** 47–51.

Kreyling, W. G., Semmler, M., Erbe, F., Mayer, P., Takenaka, S., Schulz, H., Oberdörster, G., and Ziesenis, A. (2002). Translocation of ultrafine insoluble iridium particles from lung epithelium to extrapulmonary organs is size dependent but very low. *J. Toxicol. Environ. Health A* **65,** 1513–1530.

Kreyling, W. G., Semmler-Behnke, M., and Moller, W. (2005). Ultrafine particle-lung interactions: does size matter? *J. Aerosol. Med.* **19,** 74–83.

Kubota, R., Tahara, M., Shimizu, K., Sugimoto, N., Hirose, A., and Nishimura, T. (2009). Development of a liquid chromatography-tandem mass spectrometry method for the determination of fullerene C60 and C70 in biological samples (in Japanese). *Bull. Natl. Inst. Health Sci.* **127,** 65–68.

Kuempel, E. D., Tran, C. L., Bailer, A. J., Smith, R. J., Dankovic, D. A., and Stayner, L. T. (2001). Methodological issues of using observational human data in lung dosimetry models for particulates. *Sci. Total Environ.* **274,** 67–77.

Lehnert, B. E., and Morrow, P. E. (1985a). Association of Fe-59 oxide with alveolar macrophages during alveolar clearance. *Exp. Lung Res.* **9,** 1–16.

Lehnert, B. E., and Morrow, P. E. (1985b). The initial lag in phagocytic rate by macrophages in monolayer is related to particle encounters and binding. *Immunol. Invest.* **14,** 515–521.

Madl, A. K., Wilson, D. W., Segall, H. I., and Pinkerton, K. E. (1998). Alteration in lung particle translocation, macrophage function, and microfilament arrangement in monocrotaline-treated rats. *Toxicol. Appl. Pharmacol.* **153,** 28–38.

Möller, W., Felten, K., Sommerer, K., Scheuch, G., Meyer, G., Meyer, P., Häussinger, K., and Kreyling, W. G. (2008). Deposition, retention, and translocation of ultrafine particles from the central airways and lung periphery. *Am. J. Respir. Crit. Care Med.* **177,** 426–432.

Morimoto, Y., Hirohashi, M., Ogami, A., Oyabu, T., Myojo, T., Nishi, K., Kadoya, C., Todoroki, M., Yamamoto, M., Murakami, M., *et al.* (2010). Inflammogenic effect of well-characterized fullerenes in inhalation and intratracheal instillation studies. *Part. Fibre Toxicol.* **7,** 4.

Moussa, F., Pressac, M., Genin, E., Roux, S., Trivin, F., Rassat, A., Ceolin, R., and Szwarc, H. (1997). Quantitative analysis of C_{60} fullerene in blood and tissues by high-performance liquid chromatography with photodiode-array and mass spectrometric detection. *J. Chromatogr. B Biomed. Sci. Appl.* **696,** 153–159.

Moussa, F., Trivin, F., Ceolin, R., Hadchouel, M., Sizaret, P. Y., Greugny, V., Fabre, C., Rassat, A., and Szwarc, H. (1996). Early effects of C_{60} administration in Swiss mice: a preliminary account for in vivo C_{60} toxicity. *Fullerene Sci. Technol.* **4,** 21–29.

Muhle, H., Creutzenberg, O., Bellmann, B., Heinrich, U., and Mermelstein, R. (1990). Dust overloading of lungs: investigations of various materials, species differences, and irreversibility of effects. *J. Aerosol Med.* **3,** 111–128.

Naota, M., Shimada, A., Morita, T., Inoue, K., and Takano, H. (2009). Translocation pathway of the intratracheally instilled C_{60} fullerene from the lung into the blood circulation in the mouse: possible association of diffusion and caveolae-mediated pinocytosis. *Toxicol. Pathol.* **37,** 456–462.

National Institute for Public Health and the Environment (RIVM). (2002). *Multiple Path Particle Dosimetry Model (MPPD v.1.0): A Model for Human and Rat Airway Particle Dosimetry*. Bilthoven, The Netherlands: RIVA. Report 650010030.

Naumann, B. D., and Schlesinger, R. B. (1986). Assessment of early alveolar particle clearance and macrophage function following an acute inhalation of sulfuric acid mist. *Exp. Lung Res.* **11,** 13–33.

Oberdörster, G. (1993). Lung dosimetry: pulmonary clearance of inhaled particles. *Aerosol Sci. Technol.* **18,** 279–289.

Oberdörster, G., Ferin, J., and Lehnert, B. E. (1994). Correlation between particle size, in vivo particle persistence, and lung injury. *Environ. Health Perspect.* **102,** 173–179.

Oberdörster, G., Sharp, Z., Atudorei, V., Elder, A., Gelein, R., Kreyling, W., and Cox, C. (2004). Translocation of inhaled ultrafine particles to the brain. *Inhal. Toxicol.* **16,** 437–445.

Shimada, M., Wang, W. N., Okuyama, K., Myojo, T., Oyabu, T., Morimoto, Y., Tanaka, I., Endoh, S., Uchida, K., Ehara, K., *et al.* (2009). Development and evaluation of an aerosol generation and supplying system for inhalation experiments of manufactured nanoparticles. *Environ. Sci. Technol.* **43,** 5529–5534.

Shinohara, N., Matsumoto, T., Gamo, M., Miyauchi, A., Endo, S., Yonezawa, Y., and Nakanishi, J. (2009). Is lipid peroxidation induced by the aqueous suspension of fullerene C_{60} nanoparticles in the brains of Cyprinus carpio? *Environ. Sci. Technol.* **43,** 948–953.

Xu, J. Y., Li, Q. N., Li, J. G., Ran, T. C., Wu, S. W., Song, W. M., Chen, S. L., and Li, W. X. (2007). Biodistribution of ^{99m}Tc-$C_{60}(OH)_x$ in Sprague–Dawley rats after intratracheal instillation. *Carbon* **45,** 1865–1870.